SIMULATION OF HEAT CONDUCTION AND SOOT COMBUSTION IN DIESEL PARTICULATE FILTER

K. Yamamoto[1*], M. Nakamura[1]
[1]Department of Mechanical Science and Engineering,
Nagoya University,
Furo-cho, Chikusa-ku, Nagoya, 464-8603, Japan
FAX: +81-52-789-4471
E-mail: kazuhiro@mech.nagoya-u.ac.jp
E-mail: nakamura@eess.mech.nagoya-u.ac.jp
***Corresponding author**

Keyword: numerical analysis, soot, heat conduction, diesel particulate filter, lattice Boltzmann method

Biographical notes:

Kazuhiro Yamamoto is an Associate Professor of Nagoya University. He received his BE, ME, and DE in Chemical System Engineering at the University of Tokyo in Japan. His current research field is thermal engineering, especially combustion science. His recent achievement is the development of discrete simulation for fluid dynamics including Lattice Boltzmann method and Lattice Gas Automata. In collaboration research with Los Alamos National Laboratory in the United States, numerical scheme for combustion simulation has been newly proposed, published in J. Statistical Physics. One of its applications is the diesel particulate filter (DPF), and the soot deposition and oxidation are well simulated to understand the phenomena in small-scale multiphase flow. He is a member of the Japan Society of Mechanical Engineers, the Combustion Society of Japan, the Japan Society of Fluid Mechanics, and Japan Association for Fire Science and Engineering.

Masamichi Nakamura is a mechanical engineer. He received his M. Eng. degree in 2008 from Nagoya University. His current research interests include the investigation of numerical code for porous media and soot combustion in after-treatment of diesel exhaust gas.

ABSTRACT

Recently, a diesel particulate filter (DPF) has been developed for the after-treatment of diesel exhaust gas. In simple explanation of DPF, it traps PM when exhaust gas passes its porous wall. However, since the filter would be plugged with soot particles to cause an increase of filter back-pressure, a filter regeneration process is needed. In this study, we simulated the flow with soot combustion by the lattice Boltzmann method (LBM). Here, a real filter was used in the simulation. The inner structure of the cordierite filter was scanned by a 3D X-ray CT technique. By conducting tomography-assisted simulation, we obtained local velocity and pressure distributions in the filter, which is hardly obtained by measurements. Especially, to consider the heat transfer to the solid wall of the filter substrate, the equation of heat conduction was solved, simultaneously. That is, the conjugate simulation of gas-solid flow was presented. Based on the temperature change and reaction rate in DPF, the heat and mass transfer in the filter regeneration process was discussed. (168 word)

NOMENCLATURE

c	Advection speed in LB coordinate
C_p	Heat capacity of filter
D_p	Equivalent diameter
f	Friction factor
$F_{p,\alpha}$	Distribution function of pressure
$F_{s,\alpha}$	Distribution function of temperature or species concentration
p	Pressure
Q_s	Source term by chemical reaction
R	Ideal gas constant
Re	Reynolds number
R_h	Hydraulic radius
s	Scalar of temperature or species concentration
t	Time
T	Temperature
$\boldsymbol{u}$	Velocity vector
U_{in}	Inlet velocity
W_C	Reaction rate of soot
x	Direction normal to the filter wall
y, z	Direction normal to x
Y_i	Mass fraction of species i
ε	Porosity

λ	Heat conductivity of filter substrate
ν	Kinetic viscosity
ρ	Density of mixture
ρ_s	Density of filter substrate
τ	Relaxation time

Subscript

0	Reference condition
C	Properties of soot
exit	Value at exit
in	Value at inlet
s	Properties of filter substrate
α	Number of advection speed in LB coordinate

1. INTRODUCTION

Recently, it has been reported that global warming largely affects our environment to cause climate change such as sea-level rise and coastal flooding. In order to solve the greenhouse-related problems, we need to reduce CO_2 emission in our society. Although diesel engines have an advantage of lower fuel consumption, compared with gasoline engines, there are more particulate matters (PM) including soot in exhaust gas.

To reduce these emissions especially from heavy-duty vehicles such as cargo trucks and buses, a diesel particulate filter (DPF) has been developed for the after-treatment of exhaust gas. One of the common types of DPF is a monolithic wall-flow filter. Latest researches have shown that DPF filtration efficiency can be as high as 99 % (Searles, 2002). However, the filter would be plugged with particles to cause an increase of filter back-pressure, which must be kept at lower levels, because the higher back-pressure increases fuel consumption and reduces available torque (Stamatelos, 1997). Then, a filter regeneration process is needed to oxidize accumulated particles.

There are two types of on-board and off-board regenerations. As for the off-board regeneration, DPF is periodically replaced, or cleaned to eliminate hydrocarbons and soot particles by an electric heater. The system equipped with a temperature controller, compressed air source, and combustion devices is relatively large and complicated. Thus, needless to say, it is more appropriate to use the on-board regeneration, because it is passive regeneration, and its process is spontaneously conducted during the normal engine operation. This process is called continuously regenerating trap (Cooper et al., 1997; Hawker, 1995). However, there is not

enough data, and the phenomena occurring in the filter regeneration are not well understood. This is because there are many difficulties in measurements. Typical inlet size of filter monolith is about 2 mm, and the thickness of the filter wall is only 0.2 mm, where soot particles are removed in the filter regeneration process. It is impossible to observe the small-scale phenomena inside the filter experimentally.

In this study, we simulate the flow in a real DPF by the lattice Boltzmann method (LBM). The structure of a cordierite filter is scanned by a 3D X-ray CT technique. By conducting tomography-assisted simulation, it is possible to discuss local velocity and pressure distributions in the filter, which are hardly obtained by measurements. The soot combustion is simulated to examine the filter regeneration process. The heat and mass transfer inside the filter is discussed.

2. NUMERICAL APPROACH

2.1 Lattice Boltzmann method

To simulate the flow in the gas phase, we use the lattice Boltzmann method (LBM). The fundamental idea of LBM is to construct simplified kinetic models that incorporate the essential physics of microscopic or mesoscopic processes so that the macroscopic averaged properties obey the desired macroscopic equations such as the N-S equations. The kinetic equation provides any of the advantages of molecular dynamics, including clear physical pictures, easy implementation of boundary conditions, and fully parallel algorisms (Chen and Doolen, 1998). LBM fulfills these requirements in a straightforward manner. So far, many benchmark studies have been conducted (Chen and Doolen, 1998; Yamamoto et al., 2002, Yamamoto, 2003; Yamamoto et al., 2004).

Here, we explain the numerical procedure (Yamamoto et al., 2002, Yamamoto, 2003; Yamamoto et al., 2004; Yamamoto et al., 2009; Yamamoto et al, 2010). The flow is described by the lattice BGK equation in terms of the distribution function. The evolution equation using the pressure distribution function is

$$p_\alpha(\boldsymbol{x}+\boldsymbol{c}_\alpha\delta_t,\ t+\delta_t)-p_\alpha(\boldsymbol{x},\ t)=-\frac{1}{\tau}[p_\alpha(\boldsymbol{x},\ t)-p_\alpha^{eq}(\boldsymbol{x},\ t)] \qquad (1)$$

where $c = \delta_x/\delta_t$, and δ_x and δ_t are the lattice constant and the time step, and τ is the relaxation time that controls the rate of approach to equilibrium. The equilibrium distribution function, p_α^{eq}, is given by

$$p_\alpha^{eq} = w_\alpha \left\{ p + p_0 \left[3\frac{(\boldsymbol{c}_\alpha \cdot \boldsymbol{u})}{c^2} + \frac{9}{2}\frac{(\boldsymbol{c}_\alpha \cdot \boldsymbol{u})^2}{c^4} - \frac{3}{2}\frac{\boldsymbol{u}\cdot\boldsymbol{u}}{c^2} \right] \right\} \qquad (2)$$

The sound speed, c_s, is $c/\sqrt{3}$ with $p_0 = \rho_0 R T_0 = \rho_0 c_s^2$. Here, p_0 and ρ_0 are the pressure and density in the reference conditions. In this study, to consider the variable density, we adopt the low Mach number approximation (Yamamoto et al., 2002, Yamamoto, 2003; Yamamoto et al., 2004). To validate our numerical scheme, 3D simulation in cold flow is conducted by D3Q15 model. Then, the pressure drop across the filter is simulated more precisely. Since it takes more time to simulate the combustion field, D2Q9 model is used for the 2D simulation of filter regeneration process.

The pressure and local velocity of $\boldsymbol{u}=(u_x, u_y, u_z)$ are obtained using the ideal gas equation.

$$p = \sum_\alpha p_\alpha \qquad (3)$$

$$\boldsymbol{u} = \frac{\rho_0}{\rho}\frac{1}{p_0}\sum_\alpha \boldsymbol{e}_\alpha p_\alpha \qquad (4)$$

The relaxation time is related with transport coefficients such as kinetic viscosity using $\nu = (2\tau - 1)/6\ c^2\delta_t$. Through the Chapman-Enskog procedure, the Navier-Stokes equations are derived from these equations (Chen and Doolen, 1998). The LBM formula for temperature and concentration fields is

$$F_{s,\alpha}(\boldsymbol{x}+\boldsymbol{e}_\alpha\delta_t,\ t+\delta_t) - F_{s,\alpha}(\boldsymbol{x},\ t) = -\frac{1}{\tau_s}[F_{s,\alpha}(\boldsymbol{x},\ t) - F_{s,\alpha}^{eq}(\boldsymbol{x},\ t)] + w_\alpha Q_s, \qquad s = T,\ Y_i \qquad (5)$$

where Q_s is the source term due to chemical reaction. The equilibrium distribution function, $F_{s,\alpha}^{eq}$, is

$$F_{s,\alpha}^{eq} = w_\alpha \cdot s\left\{ 1 + 3\frac{(\boldsymbol{c}_\alpha \cdot \boldsymbol{u})}{c^2} + \frac{9}{2}\frac{(\boldsymbol{c}_\alpha \cdot \boldsymbol{u})^2}{c^4} - \frac{3}{2}\frac{\boldsymbol{u}^2}{c^2} \right\} \qquad (6)$$

Temperature, T, and mass fraction of species, Y_i, are determined by these distribution functions.

$$T = \sum_\alpha F_{T,\alpha} \qquad (7)$$

$$Y_i = \sum_{\alpha} F_{Yi,\alpha} \qquad (8)$$

2.2 Heat transfer in solid phase

In the filter regeneration process, the gas phase temperature due to soot combustion becomes high to cause the heat transfer to the solid phase of filter substrate. Then, the following equation of heat conduction in 2D is solved.

$$\frac{\partial T}{\partial t} = \frac{\lambda}{\rho_s C_p}\left\{\frac{\partial^2 T}{\partial x^2} + \frac{\partial^2 T}{\partial y^2}\right\} \qquad (9)$$

where λ, ρ_s and C_p are the heat conductivity, density, and heat capacity of the filter. These values of the cordierite filter are 1.9 W/mK, 2500 kg/m^3, and 1170 J/kgK. Needless to say, the convection and chemical reaction are not included in this equation. By coupling the equations in gas phase and using appropriate boundary conditions, it is possible to solve the problem. In order to determine the temperature at the interface between gas and solid phases, it is assumed that the temperature and heat flux in the gas phase are equal to those in solid phase. Other boundary conditions are explained in the next section.

2.3 Calculation domain and X-ray CT technique

To simulate the flow in the real diesel filter, we obtain the inner structure by the 3D X-ray CT (Computed Tomography) technique (Yamamoto et al., 2009; Yamamoto et al., 2010). Non-destructive nature of the CT technique allows visualization of filter inner structure actually used. We have confirmed the applicability of the tomography-assisted simulation. In the present study, we employ a similar data processing technique.

Figure 1 shows a CT image of the filter. Three slice images of the filter are shown. The spatial resolution is 1 μm/pixel, which is the finest level in the reported CT measurements. The image area is 400 μm (x) × 400 μm (y) × 200 μm (z). The exhaust gas passes through the filter wall in the x-direction. Complex porous structure with variety of pore size is well observed. The averaged porosity of the filter is about 0.4. In the simulation of filter regeneration, two-dimensional slice image in x-y plane is used.

The calculation domain in 3D simulation is 400 μm × 100 μm × 100 μm, and the grid number is 401 (N_x)× 101 (N_y) ×101 (N_z). The grid size is 1 μm, which is the spatial resolution in X-ray CT measurement. In the combustion simulation, an over-all reaction by Lee et al. (1962) is used. For simplicity, any catalytic effects are not considered.

As for the boundary condition, the inflow boundary is adopted at the inlet (He et al., 1998). The inlet velocity of U_{in} is varied from 0.1 to 20 m/s, and the oxygen concentration of exhaust gas is changed. The gas component is of the diesel exhaust gas, and its temperature is 673 K (Yamamoto et al., 2009; Yamamoto et al., 2010). The soot mass fraction is also varied from 0.01 to 0.04. At the sidewall, the slip boundary conditions are adopted, considering the symmetry (Inamuro et al., 1999). At the outlet, the pressure is constant, and the gradient of scalar such as temperature and mass fraction is set to be zero. On the surface of the filter substrate, the non-slip boundary condition is adopted (He and Luo, 1997).

3. RESULTS AND DISCUSSION

3.1 Flow field

Before simulating the filter regeneration process, we examine the flow inside the filter. The cold flow at room temperature is used. Figure 2 shows the velocity field under steady state with small velocity perturbation. The inlet velocity is 1 m/s. The velocity vector is shown, with filter substrate by gray region. Three different slice images are shown at (a) x = 50μm, (b) x = 200μm, and (c) x = 350μm. It is found that the ceramic filter has many small pores. Then, the velocity and its direction are largely changed when the flow passes through the filter wall.

Next, we examine the pressure field inside the filter. The result is shown in Fig. 3. This pressure is the averaged value in the y-z plane. For comparison, we check the porosity, ε, in this region. The filter wall is roughly located in the range of 50 μm < x < 350 μm, and the porosity outside the filter is unity. It is well known that, in case of homogenous porous media, the pressure linearly decreases along the flow direction, and the pressure gradient is constant. However, as seen in this figure, since the porosity inside the filter wall is largely varied from 0.2 to 0.9, the pressure gradient is changed. Therefore, depending on the non-uniformity of pore-structure, both flow and pressure are changed inside the filter.

To confirm the validity of numerical scheme, simulation results are compared with the empirical equation. The idea is based on the porous media flow theory (Bird et al., 1960). First, the hydraulic radius, R_h, and the equivalent diameter of the filter substrate, D_p are determined.

$$R_h = \frac{volume\ \ available\ \ for\ \ flow}{total\ \ wetted\ \ surface} \qquad (10)$$

$$D_p = 6R_h \frac{1-\varepsilon}{\varepsilon} \qquad (11)$$

The friction factor, f, and Reynolds number, Re, are defined by

$$f = \left(-\frac{dp}{dx} \right) \frac{D_p}{\rho_0 U_{in}^2} \frac{\varepsilon^3}{(1-\varepsilon)} \qquad (12)$$

$$\mathrm{Re} = \frac{U_{in} D_p}{\nu(1-\varepsilon)} \qquad (13)$$

The empirical equation, which is called an Ergun equation, is as follows:

$$f = 150/\mathrm{Re} + 1.75 \qquad (14)$$

Here, we conduct the convergent study to confirm the proper calculation domain in tomography-assisted simulation. The following four cases are considered.

Case 1: 400 μm (x) × 40 μm (y) × 40 μm (z)
Case 2: 400 μm (x) × 60 μm (y) × 60 μm (z)
Case 3: 400 μm (x) × 80 μm (y) × 80 μm (z)
Case 4: 400 μm (x) × 100 μm (y) × 100 μm (z)

Figure 4 shows simulation results, compared with the empirical equation. The inlet velocity in case 4 is varied from 0.1 to 20 m/s, and it is 1 m/s in other three cases. For all cases, a good agreement with empirical equation is observed. Although the computational domain is limited in our tomography-assisted simulation, it is confirmed that we could discuss the heat and mass transfer in the real filter.

3.2 Soot combustion

Next, the combustion field is simulated. The calculation domain is 400 μm (x) × 100 μm (y), and the grid number is 401×101. Since the soot and oxygen are included in the inflow gas, the soot is automatically burned if the temperature is high enough. To initiate the soot combustion in the exhaust gas, the wall of the filter substrate is heated at 1200 K. Figure 5 shows the flow field with velocity vector and distributions of temperature, T [K], mass fraction of soot, Y_C, and the reaction rate, W_C [kg/m^{3}s]. Soot mass fraction at the inlet is 0.04, and inlet velocity is 0.1 m/s. The oxygen volume concentration of exhaust gas is 10%, and its mass fraction is 0.113. As described later, the steady state is achieved at t = 0.5 ms. Exhaust gas

passes through the tunnel in pore structure, and the complex flow pattern is observed. The temperature inside the filter wall is almost uniform. The soot concentration is decreased by the reaction with oxygen, and the reaction rate near the inlet is larger. Needless to say, the reaction rate locally varies, simply because the mass transfer of these reactants is different. In Fig.5(c), a part of soot is not oxidized inside the filter. That is, the filter regeneration process is not completed in this condition.

To study further, we examine the soot mass fraction at the filter exit ($Y_{C,exit}$). We monitor this value at different time steps. For comparison, the maximum temperature inside the DPF is also monitored. Results are shown in Fig. 6. Soot mass fraction at the inlet is 0.04, and inlet velocity is 0.1 m/s. Time, t, is counted after we start the simulation. As seen in this figure, the soot concentration is gradually reduced due to the soot oxidation. When the steady state is achieved, the soot concentration at the filter exit and the maximum temperature are almost constant. That is, the soot consumption rate (soot oxidation rate) is balanced with the soot supply in the inflow of exhaust gas.

Here, we focus on the oxygen concentration, which is an important parameter to control the regeneration rate (Pattas et al., 1995). In the simulation, the oxygen volume concentration is varied from 0 to 20%. The soot mass fraction at the inlet is 0.01, 0.02, and 0.04. When the soot concentration in exhaust gas is small, a part of soot is not oxidized inside the filter, because the temperature is not high enough to achieve the complete regeneration. However, when the soot mass fraction at the inlet is 0.04, the temperature inside DPF becomes higher to intensify the soot oxidation. Then, when the oxygen concentration is 20%, the soot concentration at the filter exit is completely zero. The above information is useful to develop future on–board DPF system for the after-treatment of diesel exhaust gas.

4. CONCLUSIONS

By conducting tomography-assisted simulation, we have discussed the soot oxidation in the filter regeneration process. The following results are obtained:

(1) Even in cold flow, the complex flow pattern is observed due to the non-uniformity of pore structure inside the filter. Although the calculation domain is limited, the simulation results show a good agreement with empirical equation of the Ergun equation.

(2) Based on the profiles of soot concentration and oxidation rate, it is possible to discuss the heat and mass transfer. When the soot concentration in exhaust gas is small, a part of soot is not oxidized inside the filter, because the temperature is not high enough to achieve the complete regeneration.

(3) When the soot mass fraction at the inlet is higher, the temperature inside DPF becomes

higher to intensify the soot oxidation. The soot consumption rate (soot oxidation rate) is balanced with the soot supply in the inflow of exhaust gas. As the oxygen concentration is higher, more soot is burned, showing that the exhaust oxygen concentration is an important parameter to promote regeneration rate in the after-treatment system.

ACKNOWLEDGMENTS

This work was partially supported by NEDO (New Energy and Industrial Technology Development Organization) in Japan.

REFERENCES

Bird, R.B., Stewart, W.E. and Lightfoot, E.N. (1960), *Transport phenomena*, Wiley, New York.

Chen S., and Doolen, G.D. (1998) 'Lattice Boltzmann method for fluid flows', *Annual Review of Fluid Mechanics*, Vol. 30, pp.329-364.

Cooper, B.J., Jung, H.J., and Toss, J.E. (1990), 'Treatment of diesel exhaust gas', *US Patent*, 4902487.

Hawker, P. (1995) 'Diesel emission control technology', *Platinum Metals Rev*., Vol. 39, No. 1, pp.2-8.

He, X., Chen, S., and Doolen, G.D. (1998) 'A novel thermal model for the lattice Boltzmann method in incompressible limit', *J. Comp. Phys*., Vol. 146, No. 1, pp.282-300.

He, X., and Luo, Li-Shi (1997) 'Lattice Boltzmann model for the incompressible Navier-Stokes equation', *Journal of Statistical Physics*, **88**(3/4), pp.927-944.

Inamuro, T., Yoshino, M., and Ogino, F. (1999) 'Lattice Boltzmann simulation of flows in a three-dimensional porous structure', *Int. J. Numer. Meth. Fluids*, Vol. 29, pp.737-748.

Lee, K.B., Thring, M.W., and Beer. J.M. (1962) 'On the rate of combustion of soot in a laminar soot flame', *Comb. Flame*, Vol. 6, pp.137-145.

Pattas, K.N., Stamatelos, A.M., Kougianos, K.N., Koltsakis, G.C., Pistikopoulos, P.K. (1995) 'Trap Protection by Limiting A/F Ratio During Regeneration', *SAE Technical Paper* 950366.

Searles, R.A., Bosteels, D., Such, C.H., Nicol, A.J., Andersson, J.D., and Jemma, C.A. (2002) 'Investigation of the feasibility of achieving Euro V heavy-duty emissions limits with advanced emission control systems', *FISITA World Congress*, F02E310, pp. 1-17.

Stamatelos, A.M. (1997) 'A review of the effect of particulate traps on the efficiency of vehicle diesel engines', *Energy Conversion and Management*, Vol. 38 (1), pp.83-99.

Yamamoto, K. (2003) 'LB simulation on combustion with turbulence', *International Journal of Modern Physics B*, Vol. 17(1/2), pp.197-200.

Yamamoto, K., He, X., and Doolen, G.D. (2002) ‘Simulation of combustion field with lattice Boltzmann method’, *Journal of Statistical Physics*, Vol. 107(1/2), pp.367-383.
Yamamoto, K., He, X., and Doolen, G.D. (2004) ‘Combustion simulation using the lattice Boltzmann method’, *JSME International Journal*, Series B, Vol. 47(2), pp.403-409.
Yamamoto, K., Nakamura, M., Yane, H., and Yamashita, H. (2010) ‘Simulation on catalytic reaction in diesel particulate filter’, *Catalysis Today*, Vol. 153, pp.118-124.
Yamamoto, K., Oohori, S., Yamashita, H., and Daido, S. (2009) ‘Simulation on soot deposition and combustion in diesel particulate filter’, *Proc. Comb. Inst.*, Vol. 32, pp.1965-1972.

Figure Captions

Figure 1 CT images of the filter are shown. The image area is 400 μm (x) × 400 μm (y) × 200 μm (z). Complex porous structure with variety of pore size is well observed.

Figure 2 Flow field and filter region; (a) x = 50μm, (b) x = 200μm, and (c) x = 350μm.

Figure 3 Distributions of pressure and porosity across filter wall.

Figure 4 Comparison between simulation results and the Ergun equation is shown. The calculation domain is changed in the flow simulation. The inlet velocity in case 4 is varied from 0.1 to 20 m/s, and it is 1 m/s in other three cases. For all cases, a good agreement with empirical equation is observed.

Figure 5 Profiles of (a) flow field with velocity vector, (b) temperature [K], (c) mass fraction of soot, and (d) reaction rate [kg/m^{3}s]. Soot mass fraction at the inlet is 0.04, and inlet velocity is 0.1 m/s. Heat and mass transfer in soot combustion is well visualized.

Figure 6 Soot mass fraction at filter exit and maximum temperature inside DPF are monitored at different time steps. Soot mass fraction at the inlet is 0.04, and inlet velocity is 0.1 m/s.

Figure 7 Mass fraction of soot at filter exit is examined at different oxygen concentration. The soot mass fraction at the inlet is varied.

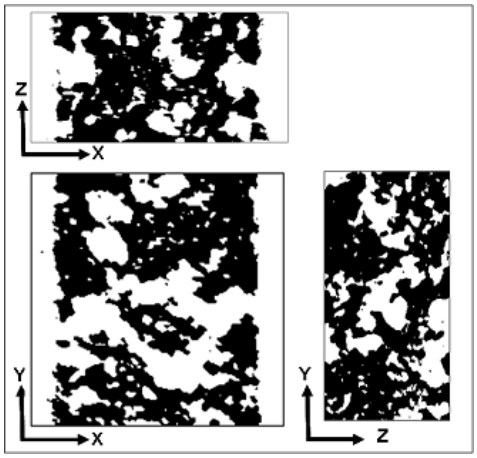

Figure 1 CT images of the filter are shown. The image area is 400 μm (x) × 400 μm (y) × 200 μm (z). Complex porous structure with variety of pore size is well observed.

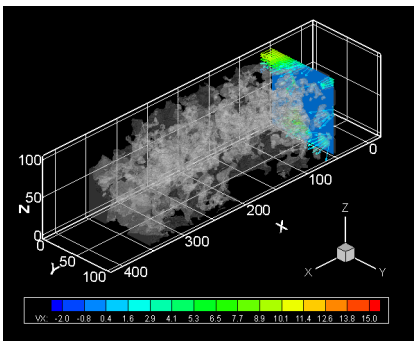

(a)

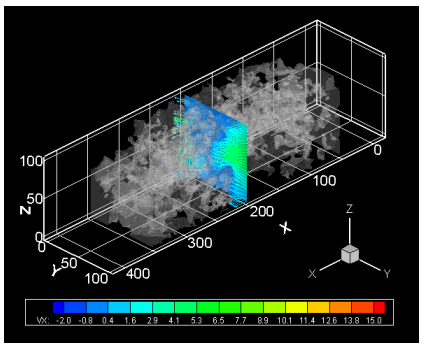

(b)

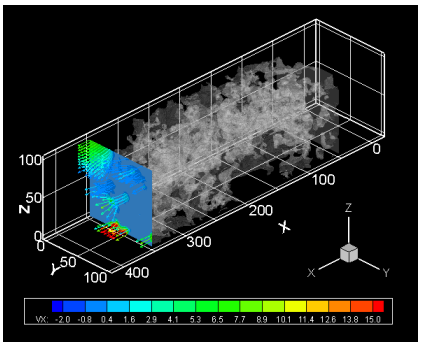

(c)

Figure 2 Flow field and filter region; (a) x = 50μm, (b) x = 200μm, and (c) x = 350μm.

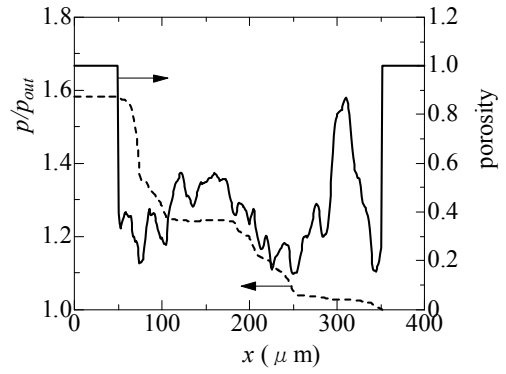

Figure 3 Distributions of pressure and porosity across filter wall.

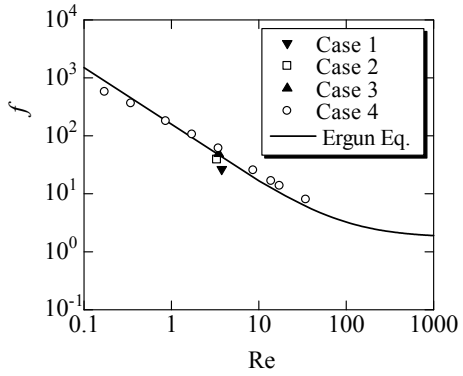

Figure 4 Comparison between simulation results and the Ergun equation is shown. The calculation domain is changed in the flow simulation. The inlet velocity in case 4 is varied from 0.1 to 20 m/s, and it is 1 m/s in other three cases. For all cases, a good agreement with empirical equation is observed.

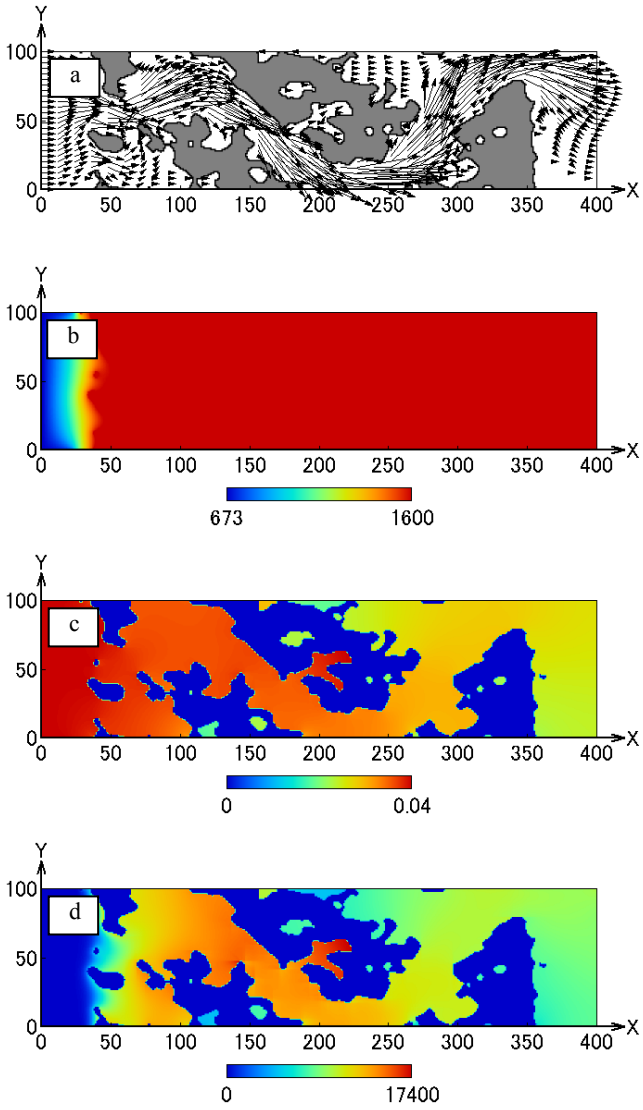

Figure 5 Profiles of (a) flow field with velocity vector, (b) temperature [K], (c) mass fraction of soot, and (d) reaction rate [kg/m^{3}s]. Soot mass fraction at the inlet is 0.04, and inlet velocity is 0.1 m/s. Heat and mass transfer in soot combustion is well visualized.

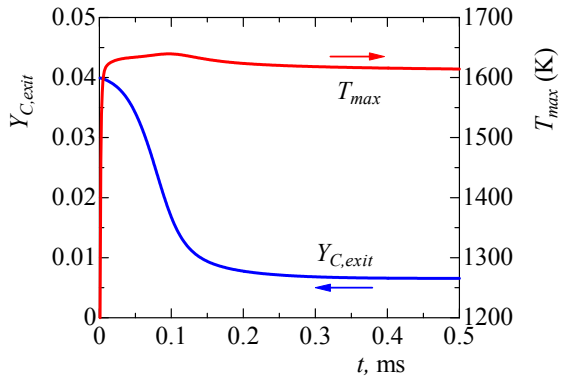

Figure 6 Soot mass fraction at filter exit and maximum temperature inside DPF are monitored at different time steps. Soot mass fraction at the inlet is 0.04, and inlet velocity is 0.1 m/s.

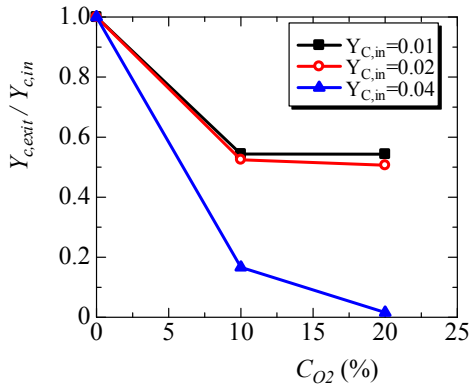

Figure 7 Mass fraction of soot at filter exit is examined at different oxygen concentration. The soot mass fraction at the inlet is varied.